High-Resolution Crystal Structures of Δ^5-3-Ketosteroid Isomerase with and without a Reaction Intermediate Analogue†

Suhng Wook Kim,‡ Sun-Shin Cha,‡ Hyun-Soo Cho,‡ Jeong-Sun Kim, Nam-Chul Ha, Moon-Ju Cho, Soyoung Joo, Kyeong Kyu Kim,§ Kwan Yong Choi, and Byung-Ha Oh*

Department of Life Science and School of Environmental Engineering, Pohang University of Science and Technology, Pohang, Kyungbuk, 790-784, South Korea

Received June 27, 1997; Revised Manuscript Received September 5, 1997⊗

ABSTRACT: Bacterial Δ^5-3-ketosteroid isomerase (KSI) catalyzes a stereospecific isomerization of steroid substrates at an extremely fast rate, overcoming a large disparity of pK_a values between a catalytic residue and its target. The crystal structures of KSI from *Pseudomonas putida* and of the enzyme in complex with equilenin, an analogue of the reaction intermediate, have been determined at 1.9 and 2.5 Å resolution, respectively. The structures reveal that the side chains of Tyr^{14} and Asp^{99} (a newly identified catalytic residue) form hydrogen bonds directly with the oxyanion of the bound inhibitor in a completely apolar milieu of the active site. No water molecule is found at the active site, and the access of bulk solvent is blocked by a layer of apolar residues. Asp^{99} is surrounded by six apolar residues, and consequently, its pK_a appears to be elevated as high as 9.5 to be consistent with early studies. No interaction was found between the bound inhibitor and the residue 101 (phenylalanine in *Pseudomonas testosteroni* and methionine in *P. putida* KSI) which was suggested to contribute significantly to the rate enhancement based on mutational analysis. This observation excludes the residue 101 as a potential catalytic residue and requires that the rate enhancement should be explained solely by Tyr^{14} and Asp^{99}. Kinetic analyses of Y14F and D99L mutant enzymes demonstrate that Tyr^{14} contributes much more significantly to the rate enhancement than Asp^{99}. Previous studies and the structural analysis strongly suggest that the low-barrier hydrogen bond of Tyr^{14} (>7.1 kcal/mol), along with a moderate strength hydrogen bond of Asp^{99} (∼4 kcal/mol), accounts for the required energy of 11 kcal/mol for the transition-state stabilization.

KSI from *Pseudomonas testosteroni* catalyzes the allylic isomerization of a variety of Δ^5-3-ketosteroids to Δ^4-3-ketosteroids by a stereospecific intramolecular transfer of the 4β-proton to the 6β-position [1] (Batzold *et al*., 1976). The enzyme, a homodimer in solution, is one of the most proficient enzymes, enhancing the catalytic rate by a factor of 11 orders of magnitude (Radzicka & Wolfenden, 1995). It has been a subject of intensive research for more than 30 years as a prototype for studying the enzyme mechanism of the allylic rearrangement. The reactions of this type are catalyzed by a wide spectrum of enzymes, such as chorismate mutase, triosephosphate isomerase, and phosphoglucoisomerase (Schwab & Henserson, 1990). Site-directed mutagenesis and kinetic studies (Holman & Benisek, 1994; Xue *et al*., 1991a,b) have identified two residues critical for the catalysis. One is Asp^{38} (*P. testosteroni* KSI numbering for all the residues throughout the text), which serves as the general base abstracting the 4β-proton of the steroid substrate, and the other is Tyr^{14} functioning as the general acid protonating or providing a hydrogen bond (H-bond) to the dienolate intermediate in the isomerization reaction:

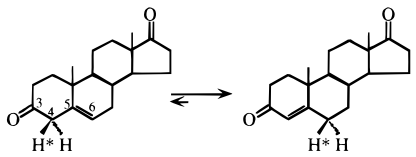

(1)

A major mechanistic enigma in the enzyme mechanisms of KSI and of many other enzymes is how a strong acid enzymatic group serves as a general base to abstract a proton from a much weaker acid group in a substrate, or vice versa. For example, the pK_a of Asp^{38} in KSI and that of the 4β-proton of the steroid substrate are 4.7 and 12.7, respectively (Hawkinson *et al*., 1994). This large disparity of pK_a values requires about 11 kcal/mol for transition-state stabilization, which coincides with the experimentally observed value (Hawkinson *et al*., 1991). A conventional account for these energies is formation of multiple favorable interactions of moderate strength at the active site (Shan *et al*., 1996). For KSI, 3−4 such H-bonds would be necessary to account for the required energy, but Tyr14 has been the only residue known to provide a H-bond to the reaction intermediate. As an alternative account, formation of a short, very strong (low-barrier) hydrogen bond (LBHB) between a catalytic group and a reaction intermediate was proposed to take place in KSI and other enzymes including several isomerases, serine proteases, hydrolases, and lyases (Cleland & Kreevoy, 1994; Frey *et al*., 1994). It has been suggested that when pK_as of two oxygens involved in the H-bond are similar, the

† The coordinates have been deposited with the Brookhaven Protein Data Bank [codes 1OPY for the enzyme and 4TST for the enzyme/equilenin complex]. This study made use of the X-ray Facility at Pohang Light Source and was supported by the Basic Science Research Fund of POSTECH and in part by the Non-Directed Research Fund, Korea, and by the Research Center for New Bio-Materials.

* To whom correspondence should be addressed: (Tel) 82-562-279-2289; (Fax) 82-562-279-2199; (e-mail) bhoh@vision.postech.ac.kr.

‡ These three authors contributed equally to this work.

§ Present address: Department of Chemistry, University of California−Berkeley, Berkeley, CA 94720.

⊗ Abstract published in *Advance ACS Abstracts,* November 1, 1997.

S0006-2960(97)01546-8 CCC: $14.00

hydrogen can be equally shared, and its bonding to both the oxygens becomes essentially covalent as the two oxygens become closer (Cleland & Kreevoy, 1994). As proposed, the covalent character could provide a large energetic contribution to the strength of the LBHB (some 10−20 kcal/mol) while ordinary H-bond strength is mainly electrostatic. Recently, however, the special energetic contribution at $\Delta pK_a = 0$ has been disputed experimentally, showing that the H-bond energy is only linearly correlated with ΔpK_a, being maximum at $\Delta pK_a = 0$ (Shan *et al*., 1996) and by *ab initio* calculation showing no special stabilization associated with the matched pK_as (Scheiner & Kar, 1995). In organic solvent, low fractionation factors for the deuterium exchange of H-bonds (Loh & Markley, 1994) and unusually deshielded ^{1}H NMR chemical shifts (17−22 ppm) have been detected for a number of H-bonds between two groups with an equal pK_a, in such cases as phthalate monoanions, maleate monoanions, and cyclic diamines (Frey *et al*., 1994). So far, the characteristic resonances from the simple compounds have been observed only in the absence of water and other alternative H-bonding possibilities. The resonance position of the acidic proton in hydrogen maleate shifted 8 ppm upfield from 20 ppm when H-bonding imidazolium counterion was introduced into the solution (Frey *et al*., 1994). Recently, a highly deshielded ^{1}H resonance at 18.15 ppm was found when dihydroequilenin, an analogue of the dienolate intermediate, was added to *P. testosteroni* KSI (Zhao *et al*., 1996). The resonance, disappearing in the mutant Y14F, was found in proximity to aromatic protons and exhibited a low fractionation factor (0.34), consistent with formation of an intermolecular LBHB between Tyr^{14} OH and the oxyanion of dihydroequilenin, which corresponds to the dienolate oxygen at the C3 position. The strength of the LBHB was estimated as >7.1 kcal/mol.

Structural information of KSI had been virtually lacking until the three-dimensional NMR structure (Wu *et al*., 1997) and the secondary structure (Zhao *et al*., 1997) of *P. testosteroni* KSI were reported very recently (Wu *et al*., 1997). In parallel, we have determined the crystal structures of *Pseudomonas putida* KSI and of the enzyme in complex with an analogue of the dienolate intermediate at 1.9 and 2.5 Å, respectively. The two homologous enzymes share 34% sequence identity (Kim *et al*., 1994). The overall structure is similar to the solution structure, but it is obviously different from the 6 Å crystal structure of *P. testosteroni* KSI (Westbrook *et al*., 1984). Compared with the solution structure (rms deviation of backbone atoms 1.54 ± 0.24 Å), the much more accurate 1.9 Å resolution structure of the uninhibited KSI (coordinates error for all atoms <0.3 Å) and the structure of the complex revealed all the active-site residues and their detailed interactions with the reaction intermediate analogue, leading to a conclusion that a strong LBHB and a medium-strength H-bond are the sources of 11 kcal/mol of the transition-state stabilization.

EXPERIMENTAL PROCEDURES

Protein Purification. KSI was isolated from an overexpressing *Escherichia coli* strain [BL21 (DE3)] and purified using a deoxycholate affinity column and Superose 12 column (Pharmacia) as previously described (Kim & Choi, 1995). KSI with methionine residues replaced by selenomethionine (Se-Met-KSI) was isolated in the same way from the methionine auxotrophic strain B834 (DE3) grown in a minimal medium containing selenomethionine. Mass spectrometric analysis of the Se-Met-KSI indicated that all seven methionine residues were substituted by selenomethionines with virtually 100% efficiency. D99L and D38N mutant KSI genes were constructed by the site-directed mutagenesis method using a Muta-gene *in vitro* mutagenesis kit (Bio-Rad).

Crystallization. Native KSI crystals were grown at 22 °C from 1.4 M sodium acetate and 0.1 M ammonium acetate (pH 4.6) in hanging drops. The crystals belong to the space group $C222_1$ with unit cell dimensions of $a = 36.40$, $b = 96.12$, and $c = 74.40$ Å. In this crystal form, the molecular 2-fold axis coincides with a crystallographic 2-fold axis, and one subunit of the enzyme is contained in the asymmetric unit. For the crystals of the complex, D38N mutant enzyme was used (see Results and Discussions), and the crystals were obtained by the cocrystallization method. A small amount of equilenin was dissolved in dimethyl sulfoxide, and 2 μL of the solution was mixed with 70 μL of enzyme solution (20 mg/mL). A saturating amount of equilenin was ensured by the presence of white precipitation of the compound formed immediately after mixing. The crystals of the complex were grown at 22 °C from 1.1 M sodium acetate and 0.1 M ammonium acetate (pH 4.6) in hanging drops. Although the crystallization condition is similar to that for the native crystals, the space group was $C2$ with unit cell dimensions of $a = 88.62$, $b = 72.33$, and $c = 51.18$ Å and $\beta = 90.67°$. The crystals contain one dimer in the asymmetric unit.

Data Collection, Structure Determination, and Refinement. All diffraction data were measured on a DIP2020 area detector with graphite monochromated CuKα X-rays generated by a MacScience M18XHF rotating anode generator operated at 90 mA and 50 kV at room temperature. Data reduction, merging, and scaling were accomplished with the programs DENZO and SCALEPACK (Otwinowski, 1993). Initial diffraction phases were obtained by multiple isomorphous replacement with the three heavy atom derivatives. Difference Patterson maps of the lead acetate and thimerosal derivatives were calculated, respectively, with the fast Fourier transform of the CCP4 suite (Collaborative Computational Project No. 4, 1994). One heavy atom site for each derivative was readily identified by strong Patterson peaks (>4σ) on Harker sections. The heavy atom positions were used to calculate MIR phases with MLPHARE (Otwinowski, 1991). The MIR phases revealed two and three minor sites for the lead acetate and thimerosal derivatives, respectively. The phases were also used to identify six out of seven possible selenium sites. Later, one missing site turned out to be on the first methionine residue, whose electron density was not visible. The MIR phases calculated at 2.8 Å resolution with all three derivative data had a mean figure of merit of 0.65 and were improved with real space density modification using the program DM in the CCP4 suite (Collaborative Computational Project No. 4, 1994). The final MIR map was of high quality showing virtually all side-chain electron densities except in the flexible regions. Skeletonization of the electron density map with BONES (Jones *et al*., 1989) helped with fitting a model of KSI using the program O (Jones & Kjeldgaard, 1993). The correct fitting was partly assured by the difference Fourier selenium densities corresponding to the sulfur atoms of six methionine residues. The model was refined using the X-PLOR program

Table 1: Crystal Structure Determination and Refinement Statistics

	crystal				
	native 1 (2)	KSI/equilenin	$Pb(OAc)_2$	thimerosal	Se-Met-KSI
resolution (Å)	2.15 (1.90)	2.5	2.80	22.80	2.8
R_{sym}[a] (%)	6.5 (6.1)	7.1	7.6	7.5	4.9
completeness ($F > 1\sigma$)	98.8 (96.2)	96.0	90.7	95.8	98.0
soaking concentration (mM)			10	20	
soaking times (h)			0.5	1	
R_{scale}[b] (%)			24.8	27.5	17.7
no. of sites			3	4	6
phasing power[c] (acen/cent)			(1.2/0.8)	(1.4/1.0)	(1.6/1.2)
R_{Cullis}[d] (%, acen/cent)			(0.75/0.74)	(0.71/0.68)	(0.63/0.59)
figure of merit[e]					0.65

	refinement ($F > 1\sigma$)			stereochemical quality	
	KSI (1.9 Å)	KSI/equilenin		KSI	KSI/equilenin
$R_{standard}$ (%)	19.8	19.1	rmsd bond lengths (Å)	0.01	0.015
R_{free}[f] (%)	26.7	25.6	rmsd bond angles (deg)	1.590	1.740
no. of atoms	964	977	Ramachandran plot (%)		
water molecules	37	79	most favored regions	88.2	87.7
average *B*-factor (Å^2)	27.0	28.5	additional allowed regions	10.8	11.3
			disallowed regions	1.0	1.0

[a] $R_{sym} = \sum|I_{obs} - I_{avg}|/\sum I_{obs}$. [b] $R_{scale} = \sum||F_{PH}| - |F_P||/\sum|F_P|$. [c] Phasing power = rms($\sum|F_H|/\sum|E|$), where E is the residual lack of closure error. [d] $R_{Cullis} = \sum|E|/\sum||F_{PH}| - |F_P||$. [e] Figure of merit = $\langle\sum P(\alpha)e^{i\alpha}/\sum P(\alpha)\rangle$, where α is the phase and $P(\alpha)$ is the phase probability distribution. [f] R_{free} was calculated with 5% of the data.

package (Brünger, 1992). MIR phases were abandoned at this point, and electron density maps calculated with phases derived from the refined model allowed fitting of the loop and tail regions. The residues 1, 60−61, 86−92, and C-terminal 124−125 (plus two extra residues in *P. putida* KSI) have no or very weak electron density in the maps, and except for residues 86−92, they were omitted in the final model. The structure of the complex was determined by the molecular replacement protocols in X-PLOR (Brünger, 1992) using the refined dimeric model of the uninhibited KSI. The whole procedure was straightforward, and the rigid-body refinement (20 steps of conjugate gradient minimization against reflections at 8−3.0 Å resolution) of the translation solution resulted in the *R*-factor of 27.2%. At this stage, in both the $2F_o - F_c$ and $F_o - F_c$ maps, strong flat electron density for the bound equilenin was found at the active site and guided the model building of the inhibitor. All the residues in the final structures are within the allowed regions in the Ramachandran plots except for Leu3 at the N-terminus, whose electron density is weak.

RESULTS AND DISCUSSIONS

Structure Determination. The structure of KSI was determined by the multiple isomorphous replacement (MIR) method, and the structure of the complex by the molecular replacement method (Table 1). We used D38N mutant enzyme for the structure of the complex, because it binds steroid analogues much more tightly owing to the absence of the negative charge at the residue 38 (Hawkinson *et al*., 1994). Furthermore, Asn^{38} mimics the protonated form of Asp^{38} in the transition state. With this mutant enzyme, equilenin, a potent analogue of the dienolate intermediate, was complexed and crystallized:

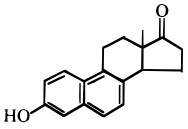

Dihydroequilenin contains -OH instead of the carbonyl O on the five-membered ring.

Protein Fold and Structural Features. The structure is reminiscent of a "coneshell" (or closed barrel) formed by a highly curved β-sheet composed of six β-strands and three α-helices (Figure 1). The α-helices are adjacent and arranged in an antiparallel orientation. The narrow end of the structure is blocked while the wide end is open to the bulk solvent forming the active-site cavity. The residues that form the secondary structures are Thr^3−Val^{20} (α-helix A1), Ile^{23}−Met^{29} (α-helix A2), Ala^{34}−Pro^{39} (β-strand B1), Pro^{44}−His^{46} (β-strand B2), Arg^{48}−Leu^{59} (α-helix A3), Val^{63}−Ser^{74} (β-strand B3), Gly^{77}−Trp^{88} (β-strand B4), Gln^{91}−Phe^{103} (β-strand B5), and Gln^{110}−Val^{123} (β-strand B6 and B7). A bulge, composed of Trp^{116}−Ser^{117}−Glu^{118}−Val^{119}, is found between strands B6 and B7. The three central antiparallel β-strands (strands B3, B4, and B5) are highly curved and span the entire monomeric structure. The curvature of strand B3 is due to a kink by the sequence of Thr^{68}−Gly^{69}−Pro^{70}. A sharp kink at Pro^{81} is responsible for the curvature of strand B4. However, the longest β-strand B5 is smoothly curved without any kink. In the solution structure of *P. testosteroni* KSI, the secondary structures are similarly defined except that residues 109 and 110, which form a loop in the crystal structure, are defined as a β-bulge (Wu *et al*., 1997).

A narrow and long patch of the β-sheet of each protomer forms a dimer interface. The dimer interactions are mostly between side chains and mostly hydrophobic. A total of 23 residues of one protomer are within 3.8 Å from the other protomer. These residues are Ala^4, Gln^5, Gln^8, Phe^{40}, Pro^{70}, Val^{71}, Arg^{72}, Ala^{73}, His^{75}, Asn^{76}, Ala^{79}, Met^{80}, Phe^{82}, Asp^{96}, Val^{97}, Ile^{98}, Val^{100}, Tyr^{115}, Trp^{116}, Ser^{117}, Glu^{118}, Val^{119}, and Asn^{120}. In addition, a string of 10 bound water molecules is found in the middle of the dimer interface, four of which mediate intersubunit H-bonds between Thr^{68}, Arg^{72}, and Asp^{96}. In contrary to the absence of main-chain H-bonds between the protomers in the solution structure of *P. testosteroni* KSI (Wu *et al*., 1997), the carbonyl oxygens of

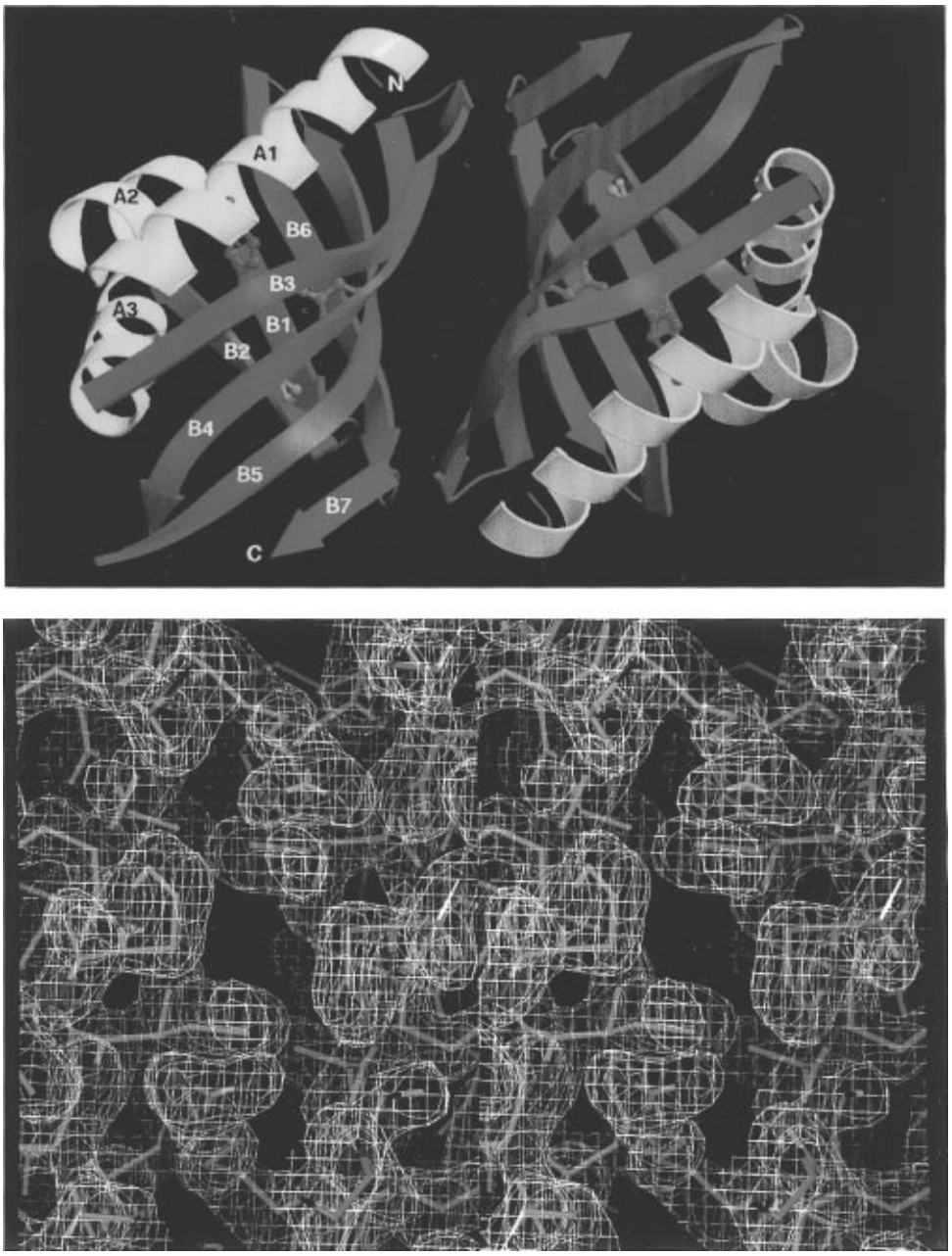

FIGURE 1: Structure of KSI. (a, top) Dimeric structure viewed roughly along the molecular 2-fold axis. The three major catalytic residues are shown in ball-and-stick model: Tyr^{14}, green; Asp^{38}, cyan; Asp^{99}, coral. The model does not contain residues 1, 60−61 between A3 and B3, and C-terminal 124−125. Strand B7 is a continuation of strand B6 considering a β-bulge between the two. (b, bottom) Stereodiagram showing the quality of the $2F_o - F_c$ electron density in the middle of the dimer interface. The carbon atoms of each of the two protomers are in green and magenta, respectively. The molecular 2-fold axis is approximately perpendicular to the picture and passes through a relatively large see-through hole surrounded by the proline and isoleucine residues. The map is contoured at 1.3σ, and calculated with the final model of KSI using data between 10 and 1.9 Å resolution. Programs Molscript (Kraulis, 1991) and Raster3D (Merritt & Murphy, 1994) were used for (a) and program O (Jones *et al*., 1989) was used for (b).

Val71, Ala73, and Val97 of one protomer are involved in H-bonds directly with the side chains of Asn^{120}, Ser^{117}, and Arg^{72} of the other protomer, respectively. In the crystal structure, only one side-chain H-bond is observed between His^{75} of one protomer and Gln^{118} of the other protomer.

A search for similar structures in the PDB data base using the computer program DALI (Holm & Sander, 1993) revealed only two, scytalone dehydratase (Lundqvist *et al*., 1994) and nuclear transport factor 2 (Bullock *et al*., 1996). Scytalone dehydratase is a trimeric protein, and nuclear transport factor 2 is a dimeric protein with a dimer interaction mode completely different from that of KSI. The folding pattern of the three enzymes is strikingly similar, although they bear no sequence or functional homology to each other. The number of proteins belonging to this novel protein fold is expected to increase.

Active-Site Residues. The structure of uninhibited KSI reveals that a cluster of three tyrosines (Tyr^{14}, Tyr^{30}, and Tyr^{55}), a bound water molecule (Wat^{504}, *B*-factor = 25.7), and Asp^{99} form a H-bonded network at the active site (Figure 2a). The catalytic residue Asp^{38} is close to Tyr^{14} and Asp^{99} but not within H-bond distance. Asp^{38} is located in the front part of the active-site cavity, while Tyr^{14} and Asp^{99} are located deeply at the back of the cavity (Figure 3). Strikingly, the residues involved in the H-bonded network are surrounded exclusively by apolar amino acids (Figure 3): Met^{11}, Ile^{15}, Leu^{17}, Val^{18}, Ile^{23}, Ile^{26}, Val^{27}, Met^{29}, Ala^{34}, Val^{36}, Ile^{45}, Ile^{51}, Phe^{54}, Leu^{59}, Ala^{65}, Met^{80}, Phe^{82}, Val^{97}, Met^{101},

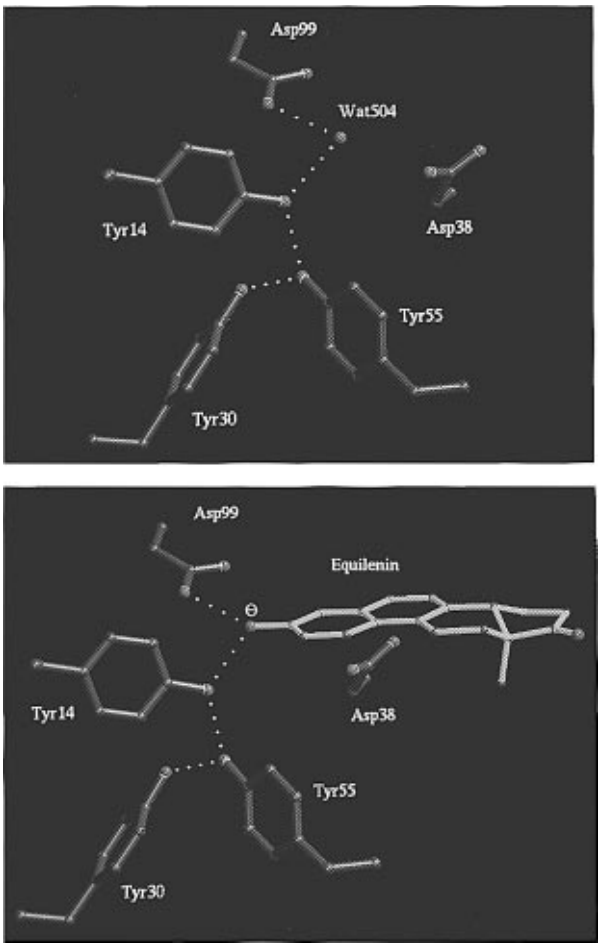

FIGURE 2: Network of H-bonds (the white dotted lines) at the active site of KSI. (a, top) Wat^{504} is a part of the network in the structure of uninhibited KSI. (b, bottom) Wat^{504} is replaced by the oxyanion of equilenin in the structure of KSI complexed with the inhibitor. Asn38 is shown as aspartic acid.

Ile^{109}, Met^{112}, and Ala^{114}. Within 4 Å of the polar atoms involved in the network, no polar atoms are found except Asp^{99} N and Ile^{98} O, which are 3.23 and 3.6 Å apart from Asp^{99} $O^{\delta 1}$, respectively. The active-site environment of *P. testosteroni* KSI must be very similar to that of *P. putida* KSI, since mapping of the primary sequence of *P. testosteroni* KSI on our structure showed that all the residues at the active-site cavity are conserved or homologously substituted. In the presence of equilenin, they are surrounded completely by apolar residues and the hydrophobic inhibitor with solvent accessibilities of zero. No water molecule is found at the active site, and thus the access of bulk solvent during the enzyme catalysis should be blocked by the layer of the apolar residues and the steroid substrate. The structure of the complex (Figure 2b) reveals that the inhibitor displaces Wat^{504} and interacts directly with Asp^{99} as well as Tyr^{14} without causing any noticeable local conformational change except the slight rotation of Asp^{38} side chain. Although an unidentified H-bonding group interacting with Tyr^{14} OH has been suggested (Austin *et al*., 1995; Holman & Benisek, 1995; Zhao *et al*., 1996), the direct involvement of Asp^{99} in the stabilization of the reaction intermediate was totally unexpected. Asp^{99} is surrounded by apolar side chains of Met^{80}, Phe^{82}, Val^{97}, Met^{101}, Met^{112}, and Ala^{114}, all protruding in the same direction from the three adjacent β-strands (Figure 4). In *P. testosteroni* KSI, the six apolar residues surrounding Asp^{99} are identical or substituted by other hydrophobic amino acids (Phe^{80}, Phe^{82}, Pro^{97}, Phe^{101}, Met^{112}, and Ala^{114}). The pK_a of Asp^{99} in this apolar environment should be elevated and appears as high as 9.5 to be consistent with the following observations: the catalytic activity of KSI decreases above pH 9.4−9.7 (Weintraub *et al*., 1970), and deprotonation of a group with a pK_a of 9.5 quenches Tyr^{14} fluorescence by 50% (Li *et al*., 1993). The unusual environment and the catalytic function of Asp^{99} strongly suggest that this residue was responsible for the observations. The high pK_a of Asp^{99} and its direct interaction with the inhibitor indicate that the bound inhibitor should be in the anion form (pK_a = 9.0) (Zhao *et al*., 1996), while Tyr^{14} OH (pK_a = 11.6) (Li *et al*., 1993) and Asp^{99} COOH are in the protonated states for favorable interactions. The stabilization of the dienolate intermediate is expected to be achieved in the same binding mode.

Tyr^{55} and Tyr^{30} involved in the H-bonded network (Figure 2) contribute not at all or only minimally to the rate enhancement. The Y55F mutant of *P. testosteroni* KSI diplayed only 4 times lower k_{cat} compared with the wild-type enzyme (Kuliopulos *et al*., 1989), consistent with the observation of no direct H bond of this residue with the bound inhibitor (Figure 2b). Tyr^{30}, replaced by phenylalanine in *P. testosteroni* KSI, also does not interact with the bound inhibitor. The Y30F mutation does not cause a detectable change in k_{cat} (unpublished result).

Participation of a LBHB. We constructed a mutant *P. putida* KSI containing an isosteric D99L substitution. The mutant enzyme exhibited a 98-fold decrease in k_{cat} compared with the wild-type enzyme. In comparison, the Y14F mutant exhibited 2000-fold decrease in k_{cat}, significantly higher than the D99L mutant. Similar results were obtained for *P. testosteroni* KSI: D99A mutation resulted in a 5000-fold decrease in *k*cat (Kuliopulos *et al*., 1989) whereas Y14F mutation caused a 50 000-fold decrease (Wu *et al*., 1997). Although the absolute values between the two sets of independent experiments are different, probably due to the difference in the measurements, the values are similar in relative scale. However, the kinetic analysis and inhibitor binding study based on the solution structure of KSI led to the conclusion that the energetic contributions of Tyr^{14} and Asp^{99} are similar in magnitude, and their H-bonds of moderate strength (4−5 kcal/mol), along with the contribution of Phe^{101} (2 kcal/mol), account for the stabilization of the bound dienolate intermediate (Wu *et al*., 1997). This conclusion is primarily based on an as-yet-unexplained catalytic role of Phe^{101}, which resulted in a reduced k_{cat} when Phe^{101} was replaced by a smaller apolar residue (e.g., 270-fold reduction by F101A mutation) (Brothers *et al*., 1995). It was also noted that the binding affinity of D99A mutant for equilenin was compared with that of Y14F mutant for a different inhibitor, estradiol. Our high-resolution structures of KSI explain the mutational effect of Phe^{101}. The residue, replaced by Met^{101} in *P. putida* KSI, is one of the residues surrounding Asp^{99} (Figure 4) and is directly below the phenyl ring of Tyr^{14}. There is no direct interaction between this residue and the bound inhibitor. When we substituted Met101 with alanine using a molecular modeling program, it was possible to place two water molecules without any steric hindrance in the empty space thus generated. One of the two water molecules makes H-bonds with the side chains of Tyr^{14} and Asp^{99} and with the other water molecule. The incorporation of water molecules at this position, which

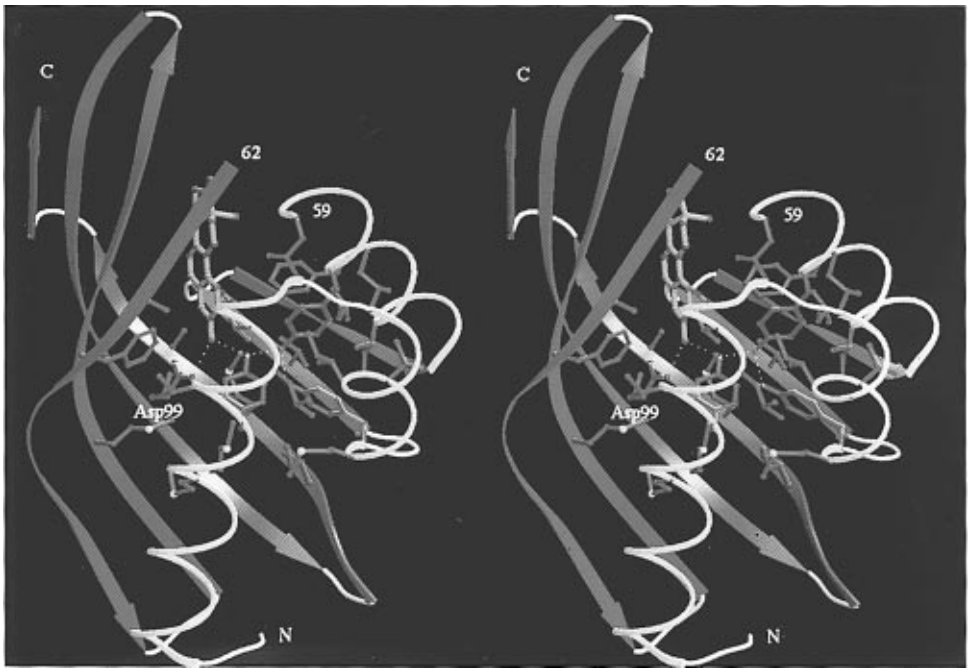

FIGURE 3: Stereodiagram showing the apolar active-site cavity of KSI in complex with equilenin. The carbon atoms of catalytic residues are in green, equilenin is in coral, and apolar residues surrounding the H-bonded network are in cyan. The H-bonds are indicated by the white dotted lines. Only Asp^{99} is labeled for clarity. The model does not contain residues 60 and 61.

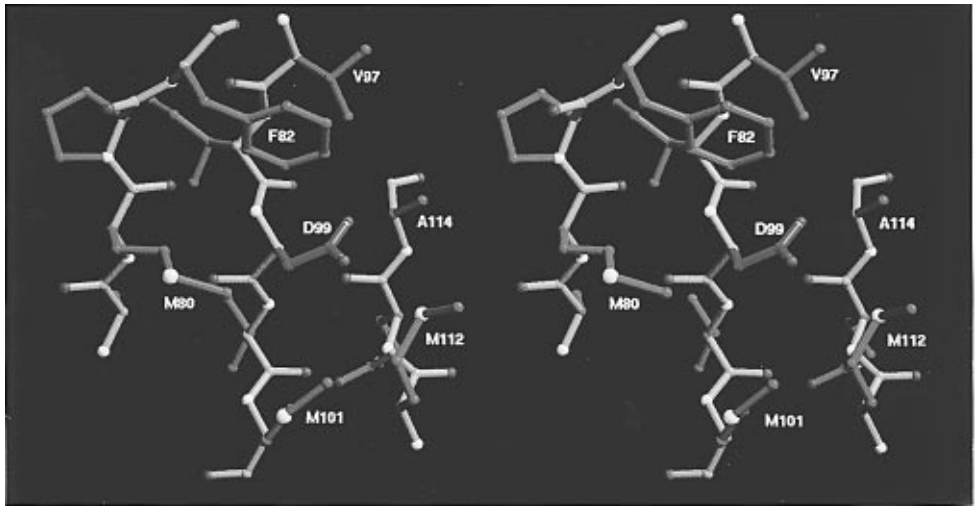

FIGURE 4: Stereodiagram showing the apolar environment of Asp^{99}. The backbone atoms in the adjacent three β-strands are in coral except for oxygens, which are in red.

should have happened in the F101A mutant, would lower the pK_a of Asp^{99} and increase the polarity of the active-site cavity, decreasing the strength of the H-bonds between the catalytic residues and the reaction intermediate. Hence, Phe101 does not contribute to the catalytic power directly, although its mutation can affect the catalysis. The 11 kcal/mol of energy has to be met solely by the two H-bonds provided by Tyr^{14} and Asp^{99}.

On the basis of the relative k_{off} values of the dienolate intermediate from Y14F and D38N mutants, the strength of the H-bond between the Tyr^{14} OH and the dienolate analogue was estimated as >7.1 kcal/mol (Zhao *et al*., 1996). This strong H-bond was assigned as the first example of an intermolecular LBHB. Although Tyr^{14} is found not to be the only residue involved in the inhibitor binding, the interpretation of the results is not affected by the new finding, because the experiment was designed to estimate the effect of Y14F mutation only. The strength of the LBHB is likely to originate from the completely apolar environment of the active site in which the pK_a of the dihydroequilenin oxyanion could be elevated and become similar to that of Tyr^{14}. A relevant model study in tetrahydrofuran has detected a strong H-bond (6.3 kcal/mol) between 4-nitrophenol and 4-nitrophenolate at $\Delta pK_a = 0$ (Shan *et al*., 1996). From this result, formation of stronger H-bonds of about 7.0 kcal/mol in a lower dielectric medium is expected to be realized. The unusual strength of the H-bond is well correlated with the highly deshielded chemical shift of the Tyr^{14} OH proton at 18.15 ppm (Zhao *et al*., 1996). Although there was a recent suggestion that the anomalous spectroscopic properties of the H-bonds are merely a reflection of similar pK_as of the two groups involved in a H-bond in the low dielectric of the protein interior (Shan *et al*., 1996), several lines of evidences in fact support that they represent the unusual strengths of H-bonds. First, all of the highly down-field-shifted ^{1}H resonances detected in the small molecular systems

or in proteins such as serine proteases (Robillard & Shulman, 1972) and aspartate aminotransferase (Kintanar *et al*., 1991) have been assigned to the protons involved in charged H-bonds, which should be stronger than neutral H-bonds. Second, such resonances have not been detected in aqueous environments in which the H-bond strength is weaker than in an apolar environment. Third, Tyr^{55} in KSI, which is engaged in the neutral H-bond with Tyr^{14}, does not display a deshielded resonance, although the two residues are both located in the apolar environment and the pK_as of the two tyrosines would be very similar.

Short distance between heteroatoms involved in a H-bond was proposed as a criterion for an LBHB (Frey *et al*., 1994). We noted that the O−O distance between the Y14 O and the equilenin O on C3 is relatively short (2.61 and 2.63 Å in the two protomers). However, because of the coordinate errors associated with the current resolution of the data (2.5 Å), meaningful measurement of the distance awaits much higher resolution data, *i.e.*, higher than 1.5 Å.

Since the kinetic analysis of the D99A or D99L mutant shows a much smaller reduction in k_{cat} than the Y14F mutant, and since Asp^{99} dose not display a deshielded chemical shift, the strength of the H-bond between Asp^{99} and the bound inhibitor should be weaker compared with the LBHB. It probably is in the medium range ($\sim$ 4 kcal/mol), considering that the bond is a charged H-bond in the apolar milieu (Scheiner & Kar, 1995). This moderate H-bond strength, along with the major contribution of the LBHB (>7.1 kcal/mol), can explain plausibly and quantitatively the requisite amount of energy for the catalytic power of KSI.

In essence, the enzyme employs a strategy of H-bond strengthening by matching the pK_as of a catalytic residue and its target and by embedding H-bonds in the apolar milieu. The only polar atoms close to the LBHB are the Tyr^{55} OH and the Asp^{99} $O^{\delta 2}$. The latter is the H-bond donor to the oxyanion of equilenin and is 4 Å apart from the Tyr^{14} OH. And finally, it is noted that the characteristic resonance of the LBHB was observed even in the presence of directly competing H-bonding donors (Asp^{99} and Tyr^{55}), in contrary to the observations in the small molecular systems (Frey *et al*., 1994). To our knowledge, this is the first detailed description of an active-site environment for the formation of an intermolecular LBHB that plays a major role in the stabilization of a reaction intermediate.

REFERENCES

Austin, J. C., Zhao, Q., Jordan, T., Talalay, P., Mildvan, A. S., & Spiro, T. G. (1995) *Biochemistry 34*, 4441−4447.

Batzold, F. H., Benson, A. M., Covey, D. F., Robinson, C. H., & Talalay, P. (1976) *Adv. Enzyme Regul. 14*, 243−267.

Brothers, P. N., Blotny, G., Qi, L., & Pollack, R. M. (1995) *Biochemistry 34*, 15453−15458.

Brünger, A. T. (1992) *X-PLOR Version 3.0*, Yale University Press, New Haven, CT.

Bullock, T. L., Clarkson, W. D., Kent, H. M., & Stewart, M. (1996) *J. Mol. Biol. 260*, 422−431.

Cleland, W. W., & Kreevoy, M. M. (1994) *Science 264*, 1887−1890.

Collaborative Computational Project No. 4 (1994) The CCP4 suite: Programs for protein crystallography, *Acta Crystallogr. D50*, 760−776.

Frey, P. A., Whitt, S. A., & Tobin, J. B. (1994) *Science 264*, 1927−1930.

Hawkinson, D. C., Eames, T. C., & Pollack, R. M. (1991) *Biochemistry 30*, 10849−10858.

Hawkinson, D. C., Pollack, R. M., & Ambulos, N. P., Jr. (1994) *Biochemistry 33*, 12172−12183.

Holm, L., & Sander, C. (1993) *J. Mol. Biol. 233*, 123−138.

Holman, C. M., & Benisek, W. F. (1994) *Biochemistry 33*, 2672−2681.

Holman, C. M., & Benisek, W. F. (1995) *Biochemistry 34*, 14245−14253.

Jones, T. A., & Kjeldgaard, M. (1993) *O version 5.9. The manual*, Uppsala University, Uppsala, Sweden.

Jones, T. A., Bergdoll, M., & Kjeldgaard, M. (1989) in *Crystallographic Computing and Modeling Methods in Molecular Design* (Bugg, C., and Ealick, S., Eds.) Springer, New York.

Kim, S. W., & Choi, K. Y. (1995) *J. Bacteriol. 177*, 2602−2605.

Kim, S. W., Kim, C. Y., Benisek, W. F., & Choi, K. Y. (1994) *J. Bacteriol. 176*, 6672−6676.

Kintanar, A., Metzler, C. M., Metzler, D. E., & Scott, R. D. (1991) *J. Biol. Chem. 266*, 17222−17229.

Kraulis, P. J. (1991) *J. Appl. Crystallogr. 24*, 946−950.

Kuliopulos, A., Mildvan, A. S., Shortle, D., & Talalay, P. (1989) *Biochemistry 28*, 149−159.

Li, Y. K., Kuliopulos, A., Mildvan, A. S., & Talalay, P. (1993) *Biochemistry 32*, 1816−1824.

Loh, S. N., & Markley, J. L. (1994) *Biochemistry 33*, 1029−1036.

Lundqvist, T., Rice, J., Hodge, C. N., Basarab, G. S., Pierce, J., & Lindqvist, Y. (1994) *Structure 2*, 937−944.

Merritt, E. A., & Murphy, M. E. P. (1994) *Acta Crystallogr. D50*, 869−873.

Otwinowski, Z. (1991) in *Isomorphous Replacement and Anomalous Scattering*; (Wolf, W. *et al*., Eds.) p 80, Science and Engineering Research Council, Warrington, U.K.

Otwinowski, Z. (1993) in *Proceedings of the CCP4 Study Weekend* (Sawyer, L., *et al*., Eds.) pp 56−62, SERC Daresbury Laboratory: Warrington, U.K.

Radzicka, A., & Wolfenden, R. (1995) *Science 267*, 90−93.

Robillard, G., & Shulman, R. G. (1972) *J. Mol. Biol. 71*, 507−511.

Scheiner, S., & Kar, T. (1995) *J. Am. Chem. Soc. 117*, 6970−6975.

Schwab, J. M., & Henserson, B. S. (1990) *Chem. Rev. 90*, 1203−1245.

Shan, S., Loh, S., & Herschlag, D. (1996) *Science 272*, 97−101.

Weintraub, H., Alfsen, A., & Baulieu, E.-E. (1970) *Eur. J. Biochem. 12*, 217−221.

Westbrook, E. M., Piro, O. E., & Sigler, P. B. (1984) *J. Biol. Chem. 259*, 9096−9103.

Wu, Z. R., Ebrahimian, S., Zawrotny, M. E., Thornburg, L. D., Perez-Alvarado, G. C., Brothers, P., Pollack, R. M., & Summers, M. F. (1997) *Science 276*, 415−418.

Xue, L., Kuliopulos, A., Mildvan, A. S., & Talalay, P. (1991a) *Biochemistry 30*, 4991−4997.

Xue, L., Talalay, P., & Mildvan, A. S. (1991b) *Biochemistry 30*, 10858−10865.

Zhao, Q., Abeygunawardana, C., Talalay, P., & Mildvan, A. S. (1996) *Proc. Natl. Acad. Sci. U.S.A. 93*, 8220−8224.

Zhao, Q., Abeygunawardana, C., & Mildvan, A. S. (1997) *Biochemistry 36*, 3458−3472.

BI971546+